

Supporting Information

Cortesi et al. 10.1073/pnas.1417803112

SI Materials and Methods

Study Species. This study included 97 fish species, of which molecular data for 44 species were available from public databases (Table S1), and 53 species were sequenced specifically for this study; 38 species were part of the teleost/Acanthomorpha whole-genome sequencing project at the Centre for Ecological and Evolutionary Synthesis, and 12 samples were obtained from the aquarium trade to be newly sequenced. Fin clips of seven species from the aquarium trade were preserved in 95% ethanol (95:5, ethanol:ddH₂O) until total DNA was extracted using a QiaGen DNeasy Tissue commercial kit (www.qiagen.com), and of the remaining five species, retinas were preserved in RNAlater (www.lifetechnologies.com) for subsequent transcriptome sequencing (Table S1). Three dotyback species (Pseudochromidae) were caught at Lizard Island (14°40' S, 145°27' E), Great Barrier Reef, Australia between 2007 and 2013 (Table S1). Dotybacks were collected on snorkel from shallow reefs (depth of 2–5 m) surrounding the island using an anesthetic clove oil solution (10% clove oil, 40% ethanol, and 50% seawater) and hand nets. A fin clip was preserved in 95% ethanol (95:5, ethanol:ddH₂O) until total DNA was extracted using a standard salt precipitation protocol (1). In addition, several dusky dotyback (*Pseudochromis fuscus*) tissues were preserved on RNAlater for subsequent transcriptome sequencing and gene expression analysis. Larval dusky dotybacks were caught overnight using light traps during the summer recruitment pulses in November of 2007 and October and November of 2013 and either directly used for MSP measurements or kept on RNAlater for subsequent gene expression analysis.

SWS2 Gene Synteny.

Transcriptome sequencing and SWS2 reference mapping. Total RNA from various dusky dotyback tissues was extracted using a QiaGen RNeasy Plus Universal Kit (QiaGen); skin, liver, eyes, and gonads from a brown male individual [total length (TL) = 69 mm]; skin, brain, anal fin, caudal fin, and gonads from a yellow female individual (TL = 71 mm); and one entire small immature individual (TL = 22 mm). BioAnalyzer (www.genomics.agilent.com) was used to measure the initial concentration of the different extracts, after which they were diluted to the same concentration and pooled. The pool was then used to prepare a library for high-throughput sequencing using the Dynabeads mRNA Purification Kit (LifeTechnologies) for mRNA selection and the Ion Total RNA-Seq Kit (LifeTechnologies) for standard steps, such as RNA-to-cDNA transcription and size selection. Transcriptome sequencing was performed on an IonTorrent PGM platform (LifeTechnologies) using a 316 chip, standard run conditions, and a 120-bp length restriction. The run produced >3.4 million unique reads (70% efficiency) with a mean length of 113 bp, equaling a total number of 389.06 Mbp, of which 330.67 Mbp had a Phred quality score of Q20 or higher (i.e., >99% base call accuracy). Subsequent quality filtering of reads was performed on the Galaxy online web server (usegalaxy.org). Data were initially trimmed using a sliding window approach with a window size of 20 and step size of 1, and reads were trimmed from both sides until reaching a base pair with a score of \geq Q20. Reads with a read length of zero were discarded, and the trimmed reads were filtered for quality so that 95% of a single read had an overall score of Q20 or higher (Q20/95). After quality filtering and removal of sequencing artifacts, the library contained >2.5 million reads with a mean length of 80 bp. Filtered reads were mapped against publicly avail-

able SWS2A and SWS2B coding sequences of the Nile tilapia (*Oreochromis niloticus*; Cichlidae) in Geneious v.6.0.2 (www.geneious.com) using customized sensitivity settings (index word length = 11; maximal gap size = 2,000 bp). Assembled reads with an average depth of 16 \times per gene were manually assigned to the different copies before generating their consensus. The resulting sequences were scored for similarity to publicly available genes using BLASTN (www.ncbi.nlm.nih.gov/BLAST). This approach produced three distinct gene products, which were thereafter used as references for mapping of orthologous genes (see below). To verify the synteny of the dusky dotyback SWS2 copies, we furthermore sequenced the genomic region containing the three genes using a combination of long-amplicon sequencing on IonTorrent and Sanger sequencing (see below). The dusky dotyback transcriptome is made available on the short-read archive database in GenBank (www.ncbi.nlm.nih.gov/genbank) (Table S1).

Additionally, we used a HiSeq 2000 DNA sequencer from Illumina (www.illumina.com) to generate retina-specific transcriptomes for five species of labrids (Labridae) and cardinalfishes (Apogonidae) (Table S1). Raw reads from these approaches were then mapped against the dusky dotyback SWS2 genes in Geneious v.6.0.2 (average depth of 250–2,500 \times per SWS2 gene), and genes were extracted as previously described for the dusky dotyback.

Public data mining. Whole-genome sequences of 24 species and the transcriptome sequences of 1 species (*Tripterygion delaisi*; average depth of 360–620 \times per SWS2 gene) were accessed from the Ensembl Genome browser (www.ensembl.org) or the Assembly (assembled contigs or scaffolds) and the short-read archive databases in GenBank (Table S1). Initially, the raw reads from unassembled datasets were mapped against SWS2 exons from the three dusky dotyback SWS2 genes in Geneious v.6.0.2 using medium-sensitivity settings (70% identity threshold for mapping) to efficiently recover all SWS2 copies. Matching reads were then manually split by copies (if more than one gene copy was present in the species) and de novo assembled, and their consensus was used as a species-specific reference for subsequent low-sensitivity mapping (only reads over 90% sequence identity map) in Geneious v.6.0.2. During this cyclic mapping, unassembled reads were mapped repeatedly against the prolonging reference (originally single exons) until the mapped regions would overlap and could be connected into an entire gene. The cyclic mapping continued the same way until the genes could not be prolonged anymore or could be connected into a genomic region (~30 kbp) that contained the highly conserved up- and downstream neighboring genes HCFC1 and LWS or GNL3L (in case of LWS loss), respectively. Alignments were continuously inspected visually to exclude ambiguous mapping of genes. In species that retained all three SWS2 paralogs, genes were interspaced by around 1,500 bp with an upstream SWS2A β , middle SWS2A α , and downstream SWS2B copy (Fig. 1).

Sequencing of the SWS2 target region. The synteny of SWS2 genes in nine species was investigated by sequencing the SWS2 target region between HCFC1 and LWS. The region was initially separated into three overlapping stretches, and universal primers were designed to amplify each stretch separately (Table S2). Long PCR was used to amplify the 5- to 13-kbp-long products using the TaKaRa LA polymerase (TaKaRa Bio Inc.; program: 35 \times 98 °C for 10 s, 60–68 °C for 1 min, and 68 °C for 20 min), and the QIAquick PCR Purification Kit (QiaGen) was used to purify the products cut from the electrophoresis gel. After purified, products were used to prepare a long-amplicon library following the

genomic DNA library preparation protocol (Ion Xpress Plus gDNA and Amplicon Library Preparation; LifeTechnologies) and sequenced on IonTorrent PGM using a 316 v2 ChIP combined with the Ion PGM Sequencing 400 Kit (LifeTechnologies). Reads were quality filtered (same as for the dusky dottyback transcriptome; see above) and de novo assembled in Geneious v.6.0.2. In several species, the consensus sequences would not cover the entire genomic region, and we, therefore, designed specific primers to sequence the missing parts by Sanger on an Applied Biosystems 3130xl Genetic Analyzer (www.appliedbiosystems.com) (Table S2). Additionally, the genomic raw reads and scaffolds of 38 species that were part of the whole-genome sequencing project at the Centre for Ecological and Evolutionary Synthesis were used to BLAST search and assemble the target SWS2 genomic region (HCFC1 upstream and LWS or GNL3L downstream) (Table S1).

SWS2 presence and synteny were assessed by mapping single exons from the dusky dottyback against the target region in Geneious v.6.0.2 using high-sensitivity settings (see above). Coding regions of SWS2 copies were subsequently extracted from the region and used for phylogenetic analyses.

Phylogenetic analyses. SWS2 coding sequences from 67 species were cut from genomic regions and combined with the transcriptome sequences from 7 species and publicly available single-gene coding sequences of 23 species (Table S1). Sequences were aligned using MAFFT v.6.8 (2), and the most appropriate model of sequence evolution was estimated in jModeltest v.2 (3) using the Akaike information criterion as the criterion for model selection. Subsequent Bayesian inference was conducted on the CIPRES platform (4) using the GTR+I+ Γ model in MrBayes v.3.2.1 (5) and a Markov chain Monte Carlo search with two independent runs and four chains each. Each run was set to 10 million generations, with trees sampled every 1,000 generations (i.e., 10,000 trees per run) with 25% of burn in after the sampling. SWS2 sequences from eel (*Anguilla anguilla*), zebrafish (*Danio rerio*), carp (*Cyprinus carpio*), and salmon (*Salmo salar* and *Oncorhynchus keta*) were used as outgroups to reconstruct phylogenetic relationships between SWS2 copies. This approach produced a partly unresolved gene tree with low phylogenetic support for SWS2 α genes in particular (Fig. S5). Consequently, to increase the phylogenetic signal, we repeated the analysis after removing the genetic regions that were affected by gene conversion (see below for gene conversion approaches) (Fig. S1).

Gene Conversion.

Single-exon phylogenies. To investigate which SWS2 copies and what genetic regions would be affected by gene conversion, we ran additional MrBayes analyses under the same conditions as mentioned above but for each exon separately (five in total) (Fig. S2).

Sliding window analysis of gene conversion. To measure the divergence between SWS2 genes, we calculated the dS (neutral process) along the coding sequences of gene copies using a sliding window strategy with a step size of 1 and a window of 30 in DNAsp v.5.10.1 (6). To avoid a bias toward clades with more representatives, we calculated the rates for one fish species per family that possesses more than one SWS2 copy. Converted regions were identified based on a sharp drop in dS between genes, which is equivalent to high sequence similarities (Fig. S3). These regions were subsequently removed from the coding sequence alignment to generate the final SWS2 gene tree (see above) (Fig. S1).

Gene resurrection: gene conversion from pseudogenes. Pseudogenes with the potential to be resurrected by converting with functional paralogs were identified in five species/lineages (Fig. 1 and Fig. S3). To test for potential gene resurrection, we ran phylogenetic analyses with the aforementioned dataset (i.e., genes without converted regions) and additionally included the converted region of the pseudogene and its functional paralog of the species

of interest (Fig. S4). Analyses were run for each species separately (i.e., a total of five analyses) in MrBayes under the same conditions as described above. Two out of five analyses were found to support the proposed gene resurrection scenario (Fig. S4).

Functional Analysis.

Neofunctionalization of SWS2 genes. Putative amino acid substitutions of importance for spectral tuning were searched for by comparing amino acid alignments of known (7) and potential key tuning sites (i.e., retinal binding pocket sites) of SWS2 genes from one fish species per family (based on alignments in ref. 8). Initially, sites were extracted based on differences in clade consensus (majority rule applied after removal of converted regions of sequences) between paralogs (Fig. S5). To identify those sites with clade specificity, we reconstructed their ancestral state (under maximal parsimony) in Mesquite v.3.0 (9). Additionally, all species were screened for the specific substitution of A269T, which is known to cause a positive shift in spectral sensitivity of 6 nm (7).

Function of the percomorph-specific SWS2A paralogs. A functional analysis of the percomorph-specific SWS2A duplication was conducted in the dusky dottyback using a combination of MSP and quantitative real-time RT-PCR (qRT-PCR) approaches.

For MSP, adult ($n = 3$) and larval ($n = 1$) dusky dottybacks were dark-adapted overnight and euthanized with an overdose of MS222 (1:2,000). Eyes were removed and dissected under IR illumination with the aid of an IR-sensitive image converter. Small pieces ($\sim 1\text{--}3\text{ mm}^2$) of retinal tissue were mounted on a no. 1 glass coverslip in a drop of PBS (410 mOsm kg^{-1} , pH 7.2) containing 4% dextran (molecular weight of 282,000; D-7265; Sigma). This preparation was covered with a smaller no. 0 coverslip, and the edges of the top coverslip were sealed with nail varnish to prevent dehydration. Absorbance spectra of individual photoreceptor outer segments were measured using a single-beam wavelength-scanning microspectrophotometer and analyzed as described in detail elsewhere (10, 11).

For qRT-PCR, RNA was extracted from retina tissues (adults) or the whole head (larvae) using TriZol following the protocol of the manufacturer (LifeTechnologies). To remove possible genomic contamination, we treated the RNA extract with DNase according to the DNA Free protocol from the manufacturer (LifeTechnologies). RNA was subsequently reverse-transcribed to cDNA using the High-Capacity RNA-to-cDNA Kit (Applied Biosystems), and the resulting concentration was measured on a NanoDrop1000 Spectrophotometer (ThermoScientific).

The relative expression of the SWS opsin genes (SWS1 and SWS2s) was quantified by qRT-PCR on a StepOnePlus Real-Time PCR System (LifeTechnologies). A 20- μL reaction volume was prepared using SYBR Green Master (Rox) dye (www.lifescience.roche.com) with a final cDNA concentration of 10 ng/ μL and a final primer concentration of 200 nM. The qRT-PCR was then performed under the following cycling conditions: 95 °C for 10 min, 40 cycles at 95 °C for 15 s, and 61 °C for 60 s. All qRT-PCR amplifications included a melt curve step after cycling. Unique primers for each opsin gene were designed with a primer specificity of $\geq 90\%$ and either the forward or the reverse primer spanning an exon-exon boundary to ensure cDNA-specific amplification of the product (60–100 bp) (Table S2). Products were furthermore sequenced by Sanger to assure accuracy of the reaction.

All primers were initially validated on a dilution series of factor 5 of a species-specific pool containing equal ratios of fragments (molarity measured on BioAnalyzer) of each of the gene copies with a starting concentration of 0.1–0.5 nM/ μL . qRT-PCR efficiencies (E_s) were calculated for each reaction from the slope of the standard curve using the equation $E = 10^{(-1/\text{slope})}$ as implemented in the StepOnePlus software (LifeTechnologies), with an efficiency of 2 being equal to 100% ($E\% = [10^{(-1/\text{slope})} - 1] - 100$) and an indicator of a robust assay. All experiments were

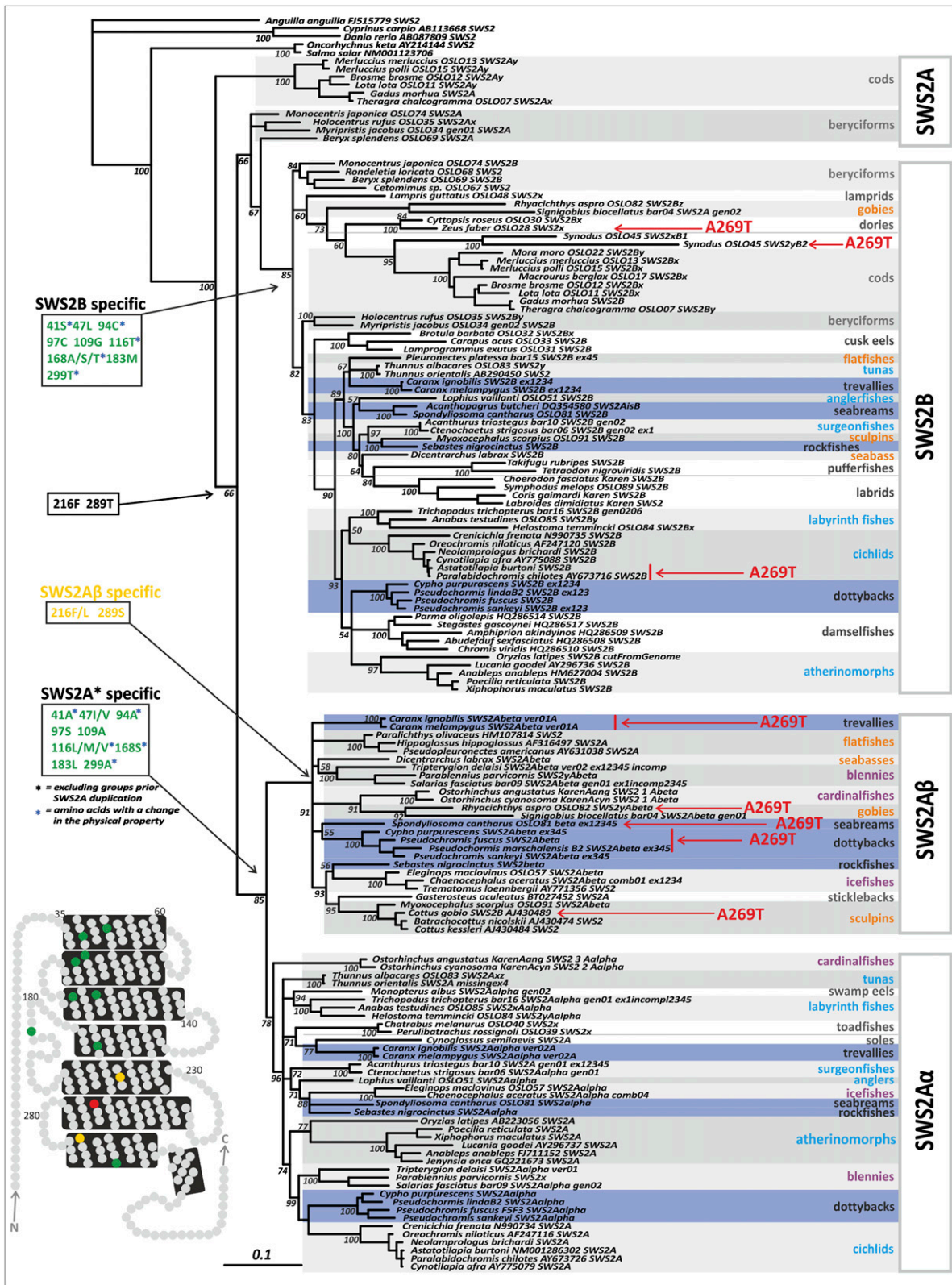


Fig. S1. SWS2 gene phylogeny and potential key amino acid substitutions. Consensus phylogeny based on the coding region of SWS2 genes without converted parts. Bayesian posterior probabilities are shown for deeper nodes (i.e., maximum one value per lineage). Lineages that retained all three SWS2 copies are shaded in blue; those with two copies are highlighted by two shades of gray. No shading means one copy retained. Common names are color-coded according to the identity of retained genes based on currently available data: blue, SWS2A α + SWS2B; orange, SWS2A β + SWS2B; violet, SWS2A α + SWS2A β . The boxes show clade-specific amino acid substitutions (as per ancestral state reconstruction; standardized to bovine rhodopsin) between SWS2A and SWS2B (green) and for SWS2A β (yellow). Amino acid substitutions that vary in physical properties are marked with blue asterisks. Species with a substitution of A269T, Legend continued on following page

which is likely to cause a positive shift in spectral sensitivity of 6 nm, are indicated with red arrows (1). *Lower Left* shows a schematic drawing of the bovine rhodopsin (based on ref. 2), with potentially important amino acid substitutions marked accordingly.

1. Yokoyama S (2008) Evolution of dim-light and color vision pigments. *Annu Rev Genomics Hum Genet* 9:259–282.
2. Palczewski K, et al. (2000) Crystal structure of rhodopsin: A G protein-coupled receptor. *Science* 289(5480):739–745.

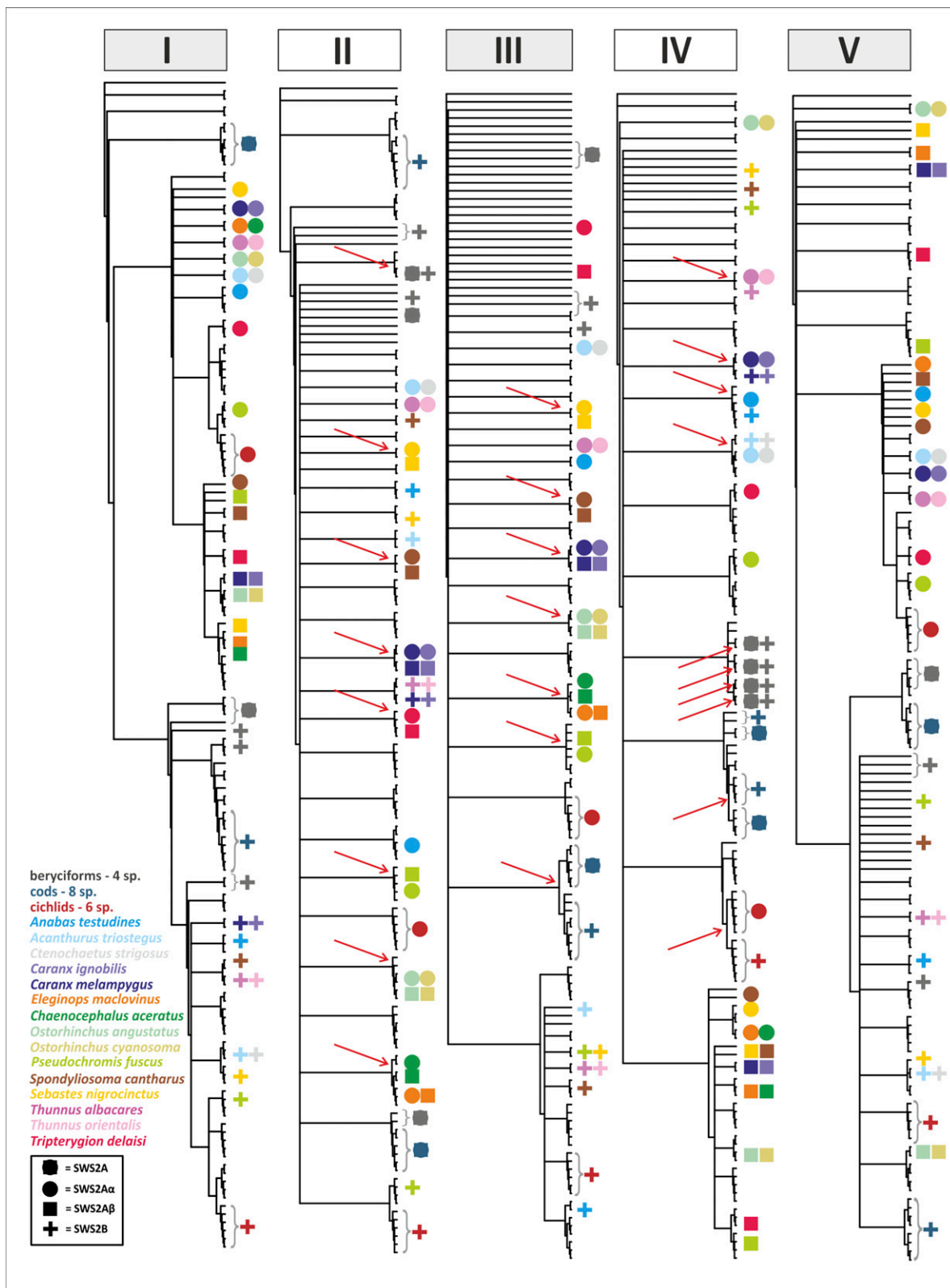


Fig. S2. Single-exon phylogenies used to identify regions under gene conversion. SWS2 copies are clustered as sisters if exons were affected by gene conversion (red arrows). Most of the conversions in exons 2 and 3 happened between SWS2A α and SWS2A β , whereas the conversions of exon 4 happened mostly between SWS2B and one of the SWS2A copies. Gene conversions of different phylogenetic age can be detected based on the tree [e.g., family-specific gene conversion in cichlids (Cichlidae; exon 4) and cods (Gadiformes; exon 3), genus-specific conversion in *Caranx* (Carangiformes; exons 2–4) and *Ostorhinchus* (Apogonidae; exons 2 and 3), or species-specific conversion in icefishes (Notothenioidei; *E. maclovinus* and *C. aceratus*; exons 2 and 3) and beryciforms (Beryciformes; exon 4)]. Note that, for beryciforms, the exon 4 of SWS2A and SWS2B always cluster as sisters within species, indicating that conversion occurred independently multiple times over in this lineage.

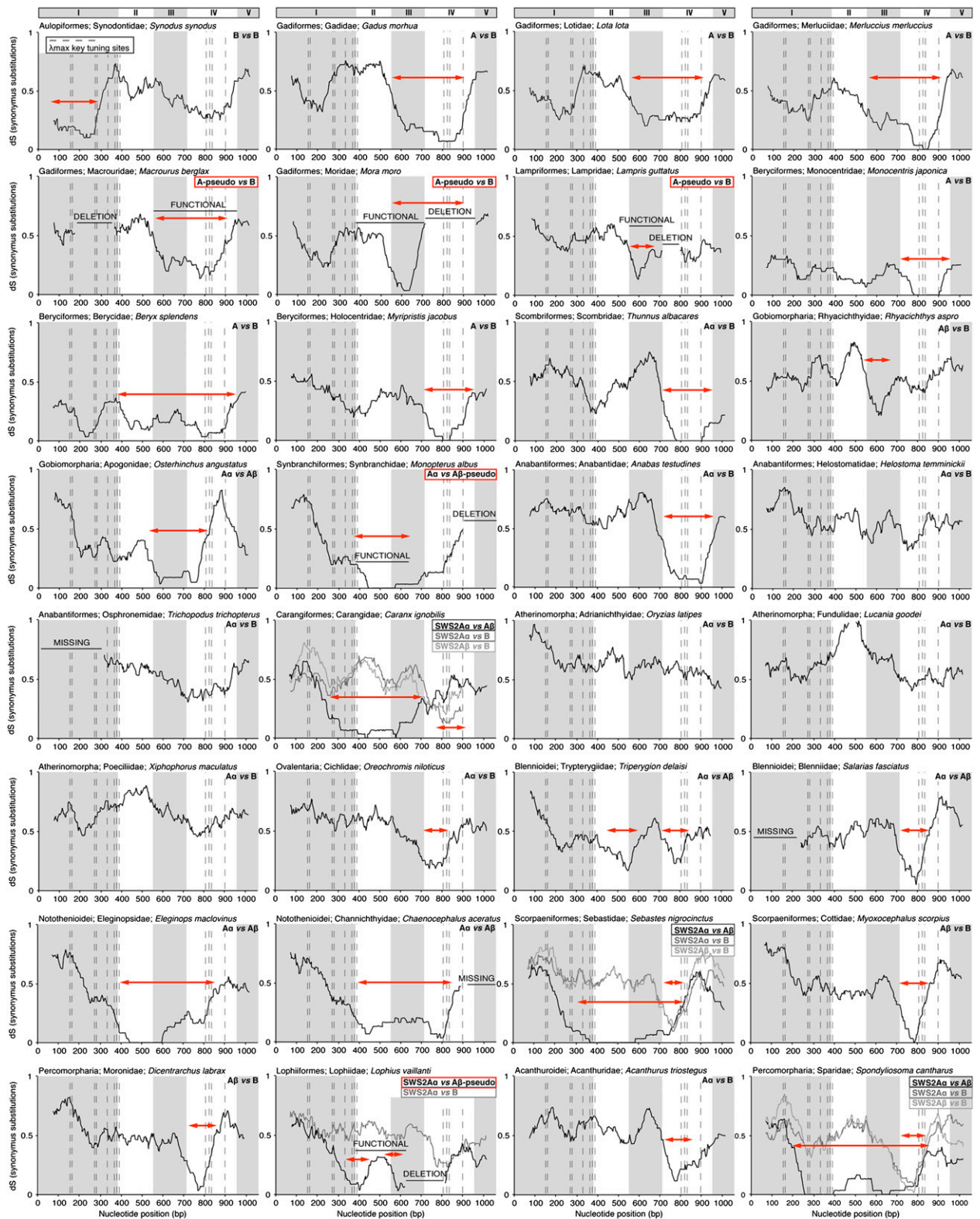


Fig. S3. Sequence comparison of SWS2 genes from one representative fish species per family. Synonymous substitution rates (dS) along gene sequences were assessed by sliding windows (size of 30 bp; step size = 1). Probable regions under gene conversion, which were removed to generate the final gene phylogeny (Fig. S1), are identified by a drop in dS and marked by red arrows. Note that, in several families, pseudogenized genes are likely to have contributed to gene conversion (framed in red) (also see Fig. S4).

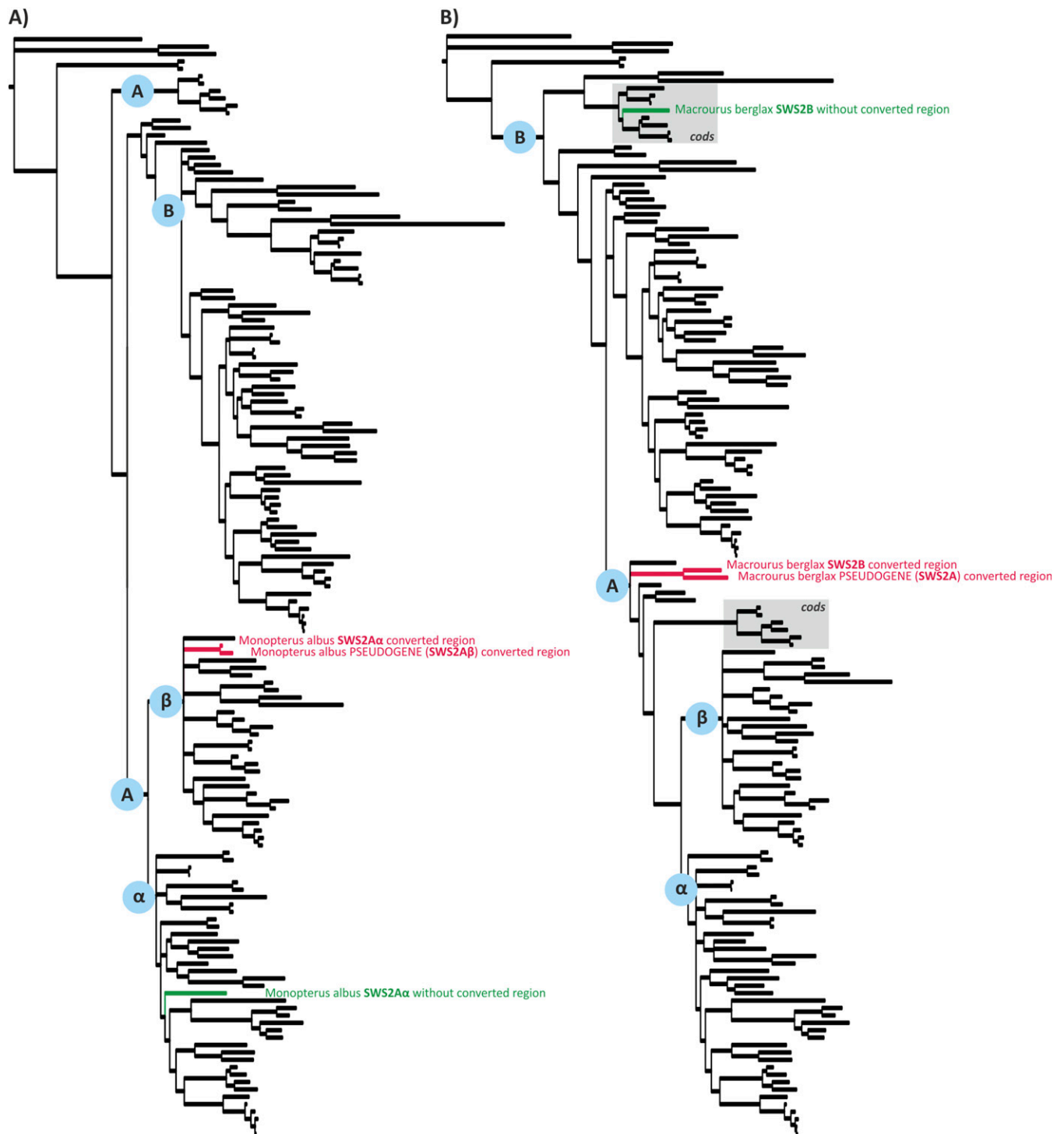


Fig. 54. Conversion from pseudogene to functional paralog potentially leading to gene resurrection. Phylogenies based on the coding genes without converted regions (all species) (similar to Fig. S1) and the converted region of the pseudogene and the target paralog (of a tested species) identified potential gene resurrection in two cases. (A) Asian swamp eel (*Monopterus albus*; Synbranchiformes). Red shows the converted regions of SWS2A α and the SWS2A β pseudogene; green shows SWS2A α without the converted region. The phylogenetic position of SWS2A α converted region in the SWS2A β clade clearly suggests the origin of the converted region in the SWS2A β pseudogene. (B) Roughhead grenadier (*Macrourus berglax*; Gadiformes). Red shows the converted regions of SWS2B and the SWSA pseudogene; green shows SWS2B without the converted region. Shaded in gray is the position of other cod species (Gadiformes).

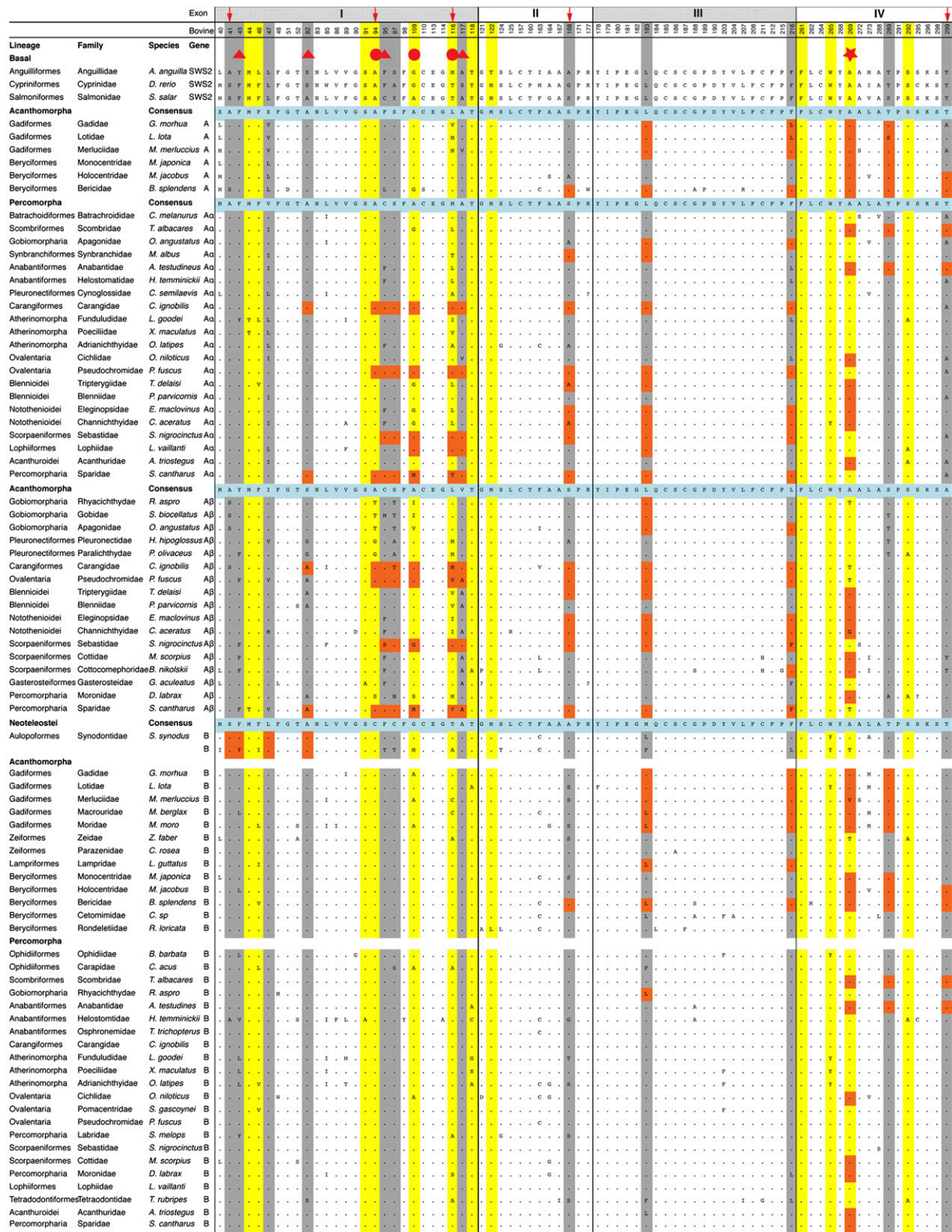


Fig. S6. SWS2 amino acid alignments (standardized to bovine rhodopsin) of known key tuning (yellow) (1) and retinal binding pocket sites. Pictured is one representative fish species per family. Highlighted in gray or marked by a red sphere are potentially functional amino acid substitutions that were identified based on clade consensus (after removing amino acids affected by conversion; orange). The red asterisk marks site 269, at which a substitution of A269T is known to cause a positive shift of 6 nm. Red triangles mark sites that did not confer to clade specificity based on an ancestral state reconstruction (after maximum parsimony). Arrows indicate those potential key substitutions that also vary in physical properties between SWS2 genes. Additional information is in Fig. S1.

1. Yokoyama S (2008) Evolution of dim-light and color vision pigments. *Annu Rev Genomics Hum Genet* 9:259–282.

Table S1. Cont.

Order	Family	Species	Source/locality	Type of data	Database	Accession no.	Blue opsins
Former Perciformes	Sparidae	<i>Spondyliosoma cantharus</i>	Teleost Genome Project	Genomic region	GenBank*	KM978043, KM978044	SW52A α + SW52A β + SW52B
Former Perciformes	Sparidae	<i>Acanthopagrus butcheri</i>	Public database	Single-gene sequence(s)	GenBank	DQ354581, DQ354580	SW52A β , SW52B

SRA, short-read archive.

*Data obtained within this study.

Table S2. Primer list for this study

Method and targeted region: gene/exon or intron	Primer name	Orientation	Primer sequence	Species
Long PCR				
HCFC1/ex1	<i>D1_DUP_HCFC1_F1</i>	Forward	CTCCTTTATAGCCACAGCTCTGTGTCC	<i>P. fuscus</i>
SWS2A β /intron1	<i>D10_fus_SWS2Abet_exinr1_R1</i>	Reverse	GTACCAAACCTCATCTTACCTCCAAGTGTG	
Long PCR				
SWS2B/ex4	<i>D6_DUP_SWS2Abet_F1</i>	Forward	GAGCGGGAGGTGACCAGGATGGTGG	<i>P. fuscus</i> , <i>T. trichopterus</i>
LWS/ex2	<i>D9_DUP_LWS_ex2_R2</i>	Reverse	CCAGTTTAGAGGRTGACGGAGTTTCTTG	<i>C. strigosus</i>
Long PCR				
SWS2A β /ex3	<i>ENDF1</i>	Forward	CCTATGTGATRTTCTCTTCTGCTTCTGCTTCG	<i>P. fuscus</i> , <i>P. sankeyi</i> , <i>P. marshallensis</i>
SWS2B/ex3	<i>BEGR1</i>	Reverse	GCAGTGCTCCTGTGGACCAGACTGGTACACCAC	<i>Cypho purpurescens</i>
Long PCR				
HCFC1/ex1	<i>D1_DUP_HCFC1_F1</i>	Forward	Sequence above	<i>A. triostegus</i>
SWS2B/ex3	<i>D16_DUP_SWS2B_ex3_R1</i>	Reverse	GTTTCATTGTTAAACTTGTTCCTGTTG	
Long PCR				
HCFC1/ex1	<i>D1_DUP_HCFC1_F1</i>	Forward	Sequence above	<i>C. strigosus</i>
SWS2B/ex3	<i>D18_DUP_SWS2B_ex1_R3</i>	Reverse	TGTATCTGAAGGCCAAGCAGTAGAAGCAG	
Long PCR				
SWS2A α /ex2	<i>D6_DUP_SWS2Abet_F1</i>	Forward	Sequence above	<i>S. biocellatus</i>
SWS2B/ex5	<i>D5_DUP_SWS2B_R2</i>	Reverse	GCAAGATTGAAGGATTTACAGCAAC	
Long PCR				
SWS2A α /ex3	<i>ENDF1</i>	Forward	Sequence above	<i>T. trichopterus</i>
SWS2B/ex3	<i>BEGR1</i>	Reverse	Sequence above	
Long PCR				
SWS2B/ex4	<i>D6_DUP_SWS2Abet_F1</i>	Forward	Sequence above	<i>S. biocellatus</i> , <i>P. platessa</i>
LWS/ex2	<i>D8_DUP_LWS_ex2_R1</i>	Reverse	CTGGTTGCAYACACTGATGGTGCTGGC	<i>A. triostegus</i>
Long PCR				
SWS2A β /ex2	<i>D6_DUP_SWS2Abet_F1</i>	Forward	Sequence above	<i>S. fasciatus</i>
SWS2A α /ex5	<i>D5_DUP_SWS2B_R2</i>	Reverse	Sequence above	
Long PCR				
SWS2A β /SWS2A α /ex1	<i>D22_DUP_beta_ex1_F1</i>	Forward	ATGAAGCACGGCCGTGTCACRGAGC	<i>S. fasciatus</i>
LWS/ex2	<i>D8_DUP_LWS_ex2_R1</i>	Reverse	Sequence above	
Long PCR				
SWS2A α /ex3	<i>D17_DUP_SWS2A_ex3_F1</i>	Forward	GACTGGTACACCACAAACAACAATAAC	<i>S. fasciatus</i>
LWS/ex2	<i>D9_DUP_LWS_ex2_R2</i>	Reverse	Sequence above	
Sanger sequencing				
SWS2A β /ex1	<i>SWS2A_betF6</i>	Forward	CATCAATGCGCTTACCG	<i>P. fuscus</i>
SWS2A β /ex4	<i>SWS2A_betR1</i>	Reverse	GAAGGAGGTGTAGGGGG	
Sanger sequencing				
SWS2B/intron3	<i>BF5_intron34</i>	Forward	CACATCTAAACTTCACCAGG	<i>P. fuscus</i>
SWS2B/ex5	<i>ABbetR6</i>	Reverse	CCCACCTTTGGAGACTTC	
Sanger sequencing				
SWS2B/ex1	<i>D27_Ctenoch_SWS2ex1_F</i>	Forward	GCGCTCTTTTATTCAATGTCAGC	<i>A. triostegus</i>
SWS2B/ex4	<i>D26_Acanth_ex4_R2</i>	Reverse	GTAGATAACAGGGTGTGTAGAC	
Sanger sequencing				
SWS2B/ex1	<i>D27_Ctenoch_SWS2ex1_F</i>	Forward	Sequence above	<i>C. strigosus</i>
SWS2B/ex4	<i>D28_Ctenoch_SWS2ex4_R</i>	Reverse	GATAACAGGGTTATAGACGGTG	
Sanger sequencing				
SWS2B/ex2	<i>D29_Tricho_ex2_F</i>	Forward	TACAGCGTAATCATCGTCAGTC	<i>T. trichopterus</i>
SWS2B/ex4	<i>D30_Tricho_ex4_R</i>	Reverse	CCACCTGTTTATTGAGGAGTATG	
Sanger sequencing				
SWS1	<i>POOL_Pfus_SWS1_F</i>	Forward	CTGTGTGCCATGGAGTCTGCC	<i>P. fuscus</i>
Pool for quantitative PCR reference	<i>SWS1_R2d_dam</i>	Reverse	TCGTTGTGGGTGTACCAGTC	
Sanger sequencing				
SWS2B	<i>POOL_Pfus_SWS2B_F</i>	Forward	GTGACTGGTACTGCCATCAATATC	<i>P. fuscus</i>
Pool for quantitative PCR reference	<i>POOL_Pfus_SWS2B_R</i>	Reverse	AACGATGGTGAAGAAGGGGATGGAA	
Sanger sequencing				
SWS2A α	<i>POOL_Pfus_SWS2Aalfa_F</i>	Forward	CTCACTATTGCATGCACCGCC	<i>P. fuscus</i>
Pool for quantitative PCR reference	<i>POOL_Pfus_SWS2Aalfa_R</i>	Reverse	GCCCATGCCAGCATCGCT	

Table S2. Cont.

Method and targeted region: gene/exon or intron	Primer name	Orientation	Primer sequence	Species
Sanger sequencing				
SWS2A β	<i>POOL_Pfus_SWS2Abeta_F</i>	Forward	CTTACCGTTGCATGCACCGTG	<i>P. fuscus</i>
Pool for quantitative PCR reference	<i>POOL_Pfus_SWS2Abeta_R</i>	Reverse	TCCACTCATCCCAGCATCTTC	
qRT-PCR				
SWS1 (efficiency: 90%)	<i>Pfus_SWS1_2F</i>	Forward	TTTTGGAGCCTTCAAGTTCACCAG	<i>P. fuscus</i>
SWS1 (efficiency: 90%)	<i>Pfus_SWS1_23R</i>	Reverse	GATGTACCTGCTCCAGCCAAAG	
qRT-PCR				
SWS2B (efficiency: 94%)	<i>Pfus_SWS2B_1F1</i>	Forward	CCGTGGGCTCCTTCACCTG	<i>P. fuscus</i>
SWS2B (efficiency: 94%)	<i>Pfus_SWS2B_12R1</i>	Reverse	GGCTCACCATGGCTCCAATC	
qRT-PCR				
SWS2A α (efficiency: 96%)	<i>Pfus_SWS2Aalfa_12F1</i>	Forward	CATGGCAACACTCGGGGTATG	<i>P. fuscus</i>
SWS2A α (efficiency: 96%)	<i>Pfus_SWS2Aalfa_2R1</i>	Reverse	CGCAAACACCAGGTGAACC	
qRT-PCR				
SWS2A β (efficiency: 96%)	<i>Pfus_SWS2Abeta_1F2</i>	Forward	GGTGAACTTGGCTGCCGCG	<i>P. fuscus</i>
SWS2A β (efficiency: 96%)	<i>Pfus_SWS2Abeta_12R1</i>	Reverse	CCATACCTCCAAGTGTGCTAC	